Synaptic mechanism underlying serotonin modulation of transition to cocaine addiction

Li, Yue; Simmler, Linda; Van Zessen, Ruud; Flakowski, Jérôme; Wan, Jin-Xia; Deng, Fei; Li, Yu-Long; Nautiyal, Katherine M; Pascoli, Vincent Jean; Luescher, Christian

How to cite

LI, Yue et al. Synaptic mechanism underlying serotonin modulation of transition to cocaine addiction. In: Science, 2021, vol. 373, n° 6560, p. 1252–1256. doi: 10.1126/science.abi9086

This publication URL: https://archive-ouverte.unige.ch/unige:158149
Publication DOI: 10.1126/science.abi9086

Synaptic mechanism underlying serotonin modulation of transition to cocaine addiction

Yue Li[1], Linda D. Simmler[1], Ruud Van Zessen[1], Jérôme Flakowski[1], Jin-Xia Wan[3,4], Fei Deng[3,4], Yu-Long Li[3,4], Katherine M. Nautiyal[5], Vincent Pascoli[1], Christian Lüscher[1,2*]

[1]Department of Basic Neurosciences, Medical Faculty, University of Geneva, CH-1211 Geneva, Switzerland.

[2]Clinic of Neurology, Department of Clinical Neurosciences, Geneva University Hospital, CH-1211 Geneva, Switzerland.

[3]State Key Laboratory of Membrane Biology, Peking University School of Life Sciences, Beijing 100871, China.

[4]PKU-IDG/McGovern Institute for Brain Research, Beijing 100871, China.

[5]Department of Psychological and Brain Sciences, Dartmouth College, Hanover, NH 03755, USA.

[*]Corresponding author. Email: christian.luscher@unige.ch

One Sentence Summary

Cocaine mediated serotonin transients cause a presynaptic depression in the dorsal striatum that prevents the potentiation of glutamate transmission responsible for compulsion in addicted individuals.

Compulsive drug use despite adverse consequences defines addiction. While mesolimbic dopamine signaling is sufficient to drive compulsion, psychostimulants such as cocaine also boost extracellular serotonin (5-HT) by inhibiting reuptake. We used SERT Met172 knockin (SertKI) mice carrying a transporter that no longer binds cocaine to abolish 5-HT transients during drug self-administration (SA). SertKI mice showed an enhanced transition to compulsion. On the other hand, pharmacologically elevating 5-HT reversed the inherently high rate of compulsion transition with optogenetic dopamine self-stimulation. The bidirectional effect on behavior was explained by presynaptic depression of orbitofrontal cortex to dorsal striatum synapses induced by 5-HT via 5-HT_{1B} receptors. Consequently, in projection-specific 5-HT_{1B} receptor knockout mice the fraction of individuals compulsively self-administering cocaine was elevated.

With chronic consumption, about 20% of cocaine users lose control and are eventually diagnosed as addicted (*1*). Increasing dopamine (DA) levels is typical of all addictive drugs (*2*), sufficient to trigger forms of synaptic plasticity underlying adaptive behaviors (*3-5*). This is exemplified by optogenetic DA neuron self-stimulation (oDASS), inducing neuronal adaptations similar to addictive drugs via selective release of DA from ventral tegmental area (VTA) neurons and yielding a bimodal distribution of compulsive and non-compulsive individuals (*6*). Cocaine also inhibits the serotonin transporter (SERT) causing 5-HT transients in the striatum. While pharmacological reduction of 5-HT in the entire forebrain can favor compulsive cocaine seeking (*7*) and differential efficacy of the 5-HT system may be involved in the vulnerability to drug addiction (*8, 9*), the relevant circuits and underlying cellular mechanisms remain elusive. To parse the locus of 5-HT modulation, we took advantage of SERT Met172 knockin (SertKI) mice carrying a transporter that does not bind cocaine without altering the basal 5-HT levels (*10-12*). Genetically encoded 5-HT sensors (Fig. S1) confirmed the absence of cocaine-evoked transients in the dorsal striatum (DS) of SertKIs (15 mg/kg i.p., Fig. 1A to C). Mice were trained to press a lever that triggered a cocaine i.v. infusion (0.5 mg/kg/infusion) accompanied by a cue light, followed by a progressive ratio (PR) session and four punishment (0.2 mA foot shock) sessions (Fig. 1D and fig. S2A). There was no difference between the SertKI and WT groups during the acquisition period (Fig. 1E). Facing punishment, however, some individuals reduced cocaine self-administration (SA), while others continued unabated (Fig. 1F). An unbiased clustering analysis integrating four behavioral parameters over the last two punishment sessions yielded two clusters: renouncers and perseverers (Fig. 1G and H). 14 out of 25 (56%) SertKI mice were classified as perseverers, in stark contrast to the 3 out of 26 (12%) in WT littermate mice (Fig. 1I). Perseverance was correlated neither to baseline cocaine SA (Fig. 1J) nor to the break point (fig. S2B), and the success rate accomplishing increasing break points did not differ between renouncers and perseverers from either genotype (Fig. 1K). Perseverers and renouncers across genotype perceived pain similarly and hot plate latency was not affected by cocaine (fig. S2C).

Next, we did the converse. We allowed mice to oDASS, which leads to compulsion in more than half of individuals (*6*) and pharmacologically elevated 5-HT levels with citalopram (Fig. 2A-C). Citalopram (10 mg/kg) induced robust 5-HT transients of magnitude comparable to cocaine (fig. S1D). Active lever presses in mice that expressed ChR2 in VTA DA neurons induced a brief train of laser stimulations (LS, see methods). All mice readily acquired oDASS (Fig. 2D) regardless of pharmacological treatment, but major differences emerged when punishment was introduced (Fig. 2E). Clustering analysis as above led to the emergence of perseverers and renouncers in both treatment groups (Fig. 2F and G). However, only 4 out of 26 (15%) citalopram treated mice were classified as perseverer, while in the saline treated group 60% were perseverers, a fraction similar to previous reports (*13*) (Fig. 2H). Again, perseverance rate was uncorrelated to baseline oDASS rate (Fig. 2I) or the break point (fig. S2D), and success rate accomplishing each break point did not differ between renouncers and perseverers across treatment groups (Fig. 2J). For all groups and condition pain perception was similar (fig. S2E).

Given that for oDASS, the synaptic potentiation of afferents from the orbitofrontal cortex (OFC) to DS drives perseverance (*13*), we wondered whether this is also the case for cocaine SA. To

selectively stimulate the OFC-DS projection, we expressed a red shifted opsin Chrimson in OFC neurons (Fig 3A) and evoked EPSCs by illuminating the terminals in brain slices of the DS 24-48 h after the last punishment session. AMPA/NMDA ratio was higher in perseverers than in renouncers of cocaine SA as well as oDASS, regardless of genotypes and treatment (Fig 3B to E), confirming that a potentiated OFC-DS pathway reflects perseverance both in oDASS and cocaine SA. In no condition were the EPSCs rectifying (fig. S3), suggesting a potentiation by an increase of the number of AMPA receptors without change in subunit composition, akin to the expression mechanism observed in individuals with compulsive oDASS (*13*).

We next examined the effect of 5-HT on synaptic transmission at the OFC-DS pathway in naïve mice. Bath application of 5-HT (4 µM) induced a presynaptic depression of excitatory transmission (Fig. 3F and G), which could be blocked by 5-HT_{1B} receptor antagonist NAS181 (20 µM), but not 5-HT_{1A} receptor antagonist WAY100635 (1 µM) (Fig. 3F and G). In line with the $G_{i/o}$ coupling of pre-synaptically located 5-HT_{1B} receptors, we observed a decreased coefficient variance ($1/CV^2$) and increased paired pulse ratio (PPR) suggesting that the presynaptic depression was expressed by a reduction of glutamate release probability (Fig. 3H and I). For confirmation, we evoked quantal events (qEPSC) after replacing extracellular calcium (Ca^{2+}) with strontium (Sr^{2+}) thus desynchronize light evoked transmitter release (*14*) and found that the qEPSC frequency decreased but the amplitude stayed unchanged (fig. S4A-C). Furthermore, 5-HT induced presynaptic depression in both D1 positive and negative neurons obtained from D1-tdTomato mice (fig. S4D), consistent with previous reports (*15-16*).

We next hypothesized that presynaptic depression may reduce the likelihood for LTP at the OFC-DS synapse, which in turn would prevent the transition to compulsion in cocaine SA. This seems plausible since chemogenetic reduction of OFC activity also reduced the fraction of perseverers in oDASS (*6*). Therefore, to establish a causal link between 5-HT induced presynaptic depression and compulsive cocaine use, we aimed to abolish 5-HT_{1B} receptors selectively in the OFC neurons targeting the DS. We injected retroAAV-ef1α-mCherry-IRES-Flpo in the DS of 5-HT_{1B} floxed mice (*17*). This led to Flpo expression in OFC neurons targeting the DS. AAV9- ef1α-fDIO-Cre or control virus was then injected in the OFC to express Cre in OFC cells targeting the DS (Fig. 4A and B), which then led to recombination and abolishment of 5-HT_{1B} receptors. We confirmed the successful receptor knockout functionally by the inability of 5-HT_{1B} agonist CP39129 (2 µM) to induce a presynaptic depression (Fig. 4C and D).

A month after virus injection, the 5-HT_{1B} knockout mice learned to self-administer cocaine (Fig. 4E). We observed an acquisition period (Fig. 4F) similar to the one described above (Fig. 1E). Once punishment was introduced, we again observed persevering and renouncing mice (Fig. 4G and H), with a higher fraction of perseverers in the projection specific 5-HT_{1B} knockout compared to control group (57% versus 13%) (Fig. 4I). Perseverance was unrelated to baseline performance (Fig. 4J), or break point in the two groups, in both control and knockout mice (Fig. 4K). The percentage of perseverers in the 5-HT_{1B} knockout group was very close to the fraction of perseverers in the SertKI group and in saline treated oDASS mice.

A synaptic mechanism thus emerges that underlies a modulatory role of 5-HT reducing the likelihood of transition to compulsion and eventually addiction (see fig. S5). In wildtype mice, cocaine binds to SERT to block 5-HT reuptake. The elevated extracellular 5-HT activates 5-HT_{1B} receptors and causes presynaptic depression of OFC terminals. This reduces the likelihood of inducing postsynaptic potentiation at OFC-DS synapses that ultimately drives compulsion. In SertKI mice, cocaine cannot bind to SERT and extracellular 5-HT remains unaffected by cocaine infusions (*10*). An OFC-DS transmission not undergoing presynaptic depression may thus enhance the likelihood to induce LTP induction and the stochastic process would then show as a higher fraction of compulsive individuals. In 5-HT_{1B} knockout mice, although cocaine still inhibits 5-HT reuptake the OFC-DS transmission is also not depressed, which again may favor LTP induction. This interpretation is in line with the report that genome-wide 5-HT_{1B} receptor knockout mice are more impulsive (*17*). These mice are also more vulnerable to cocaine (*18*), which raises the possibility that individual addiction liability may be determined by 5-HT signaling. Variation in 5-HT synthesis, synaptic release, efficiency of reuptake and extracellular levels could be additional determinants of overall vulnerability. Here we reveal addiction liability once 5-HT modulation has been eliminated, which is in line with the general idea that 5-HT opposes DA effects to inhibit behavior (*19*). However, this model is challenged by the observation that selective activation of 5-HT neurons allows to maintain high motivation in complex tasks (*20*, *21*).

While our study focused on cocaine, 5-HT may also counteract the transition to compulsion when other addictive drugs are consumed (*8, 9*). Amphetamine while having a relatively low SERT affinity increases non vesicular release of 5-HT and opioids may indirectly activate 5-HT neurons in the dorsal raphe (*22*-*24*). In fact the ratio between DAT and SERT affinity may predict the addiction liability of emerging drugs (*25*). This may also apply to natural rewards, such as food and sex, which however have low addiction liabilities, such that empirical testing will be challenging. Last but not least, it may also be interesting to explore whether 5-HT modulation levels may not only prevent the transition to compulsion, but also facilitate regaining control, as suggested by pharmacological interventions in rodents in a distinct behavioral paradigm. Forebrain 5-HT_{2C} receptors may inhibit compulsive cocaine seeking after compulsion is established (*7*), possibly via modulation of acute effects and early adaptive behaviors (*26*). By contrast, our data show that pathway specific knockout 5-HT_{1B} receptors does not affect acquisition or motivation for cocaine and specifically modulates compulsion. Three days of 5-HT_{1B} agonist (CGS12066B, 10 mg/kg, 30 min i.p. injection before each session) treatment after the last punishment session of oDASS left perseverance to oDASS intact (fig. S6), confirming that serotonin prevents transition to compulsion but cannot reverse it, once it is established.

The present mechanistic investigation may help to refine approaches to overcome the limitations and diverging findings on efficacy of 5-HT reuptake blockers in pilot studies with human addicts (*27*-*29*) or design selective agonist complementing to the empirical use of hallucinogens in addiction treatments (*30*). In summary, 5-HT emerges as a modulator of the progression to compulsion via the convergence on key synaptic mechanisms in the framework of the current circuit model for addiction (*5*).

1. M. Yucel *et al.*, *Addiction* **114**, 1095 (2019).
2. C. Lüscher, M. A. Ungless, *PLoS medicine* **3**, e437 (2006).
3. C. Lüscher, R. C. Malenka, *Neuron* **69**, 650 (2011).
4. C. Lüscher, *Ann.rev.neurosci.* **39**, 257 (2016).
5. C. Lüscher, P. H. Janak, *Ann,rev. neurosci.* **44**, 173 (2021).
6. V. Pascoli, J. Terrier, A. Hiver, C. Luscher, *Neuron* **88**, 1054 (2015).
7. Y. Pelloux, R. Dilleen, D. Economidou, D. Theobald, B. J. Everitt, *Neuropsychopharmacol.* **37**, 2505(2012).
8. L. G. Kirby, F. D. Zeeb, C. A. Winstanley, *Neuropharmacol.***61**, 421 (2011).
9. C. P. Muller, J. R. Homberg, *Behavioural brain res.* **277**, 146 (2015).
10. B. J. Thompson *et al.*, *PNAS.* **108**, 3785 (2011).
11. L. D. Simmler, R. D. Blakely, *ACS chemical neuroscience* **10**, 3053 (2019).
12. L. D. Simmler *et al.*, *Br.j.pharmacol.* **174**, 2716 (2017).
13. V. Pascoli *et al.*, *Nature* **564**, 366 (2018).
14. S. H. Oliet, R. C. Malenka, R. A. Nicoll, *Science* **271**, 1294(1996).
15. G. Dolen, A. Darvishzadeh, K. W. Huang, R. C. Malenka, *Nature* **501**, 179 (2013).
16. B. N. Mathur, N. A. Capik, V. A. Alvarez, D. M. Lovinger, *J.neurosci.* **31**, 7402 (2011).
17. K. M. Nautiyal *et al.*, *Neuron* **86**, 813(2015).
18. B. A. Rocha *et al.*, *Nature* **393**, 175 (1998).
19. Y. L. Boureau, P. Dayan, *Neuropsychopharmacol.* **36**, 74 (2011).
20. Z. Liu *et al.*, *Neuron* **81**, 1360 (2014).
21. E. Lottem *et al.*, *Nature com.* **9**, 1000 (2018).
22. P. Scholze *et al.*, *J.pharmacol. exp. ther.* **293**, 870 (2000).
23. L. D. Simmler *et al.*, *Br.j.pharmacol.***168**, 458 (2013).
24. R. Tao, S. B. Auerbach, *The J.pharmacol.exp.ther.* **303**, 704(2002).
25. M. Liechti, *Swiss medical weekly* **145**, w14043 (2015).
26. P. J. Fletcher, A. J. Grottick, G. A. Higgins, *Neuropsychopharmacol.* **27**, 576(2002).
27. S. Vayalapalli, M. Vaughn, K. Salles-Shahid, J. Byrd-Sellers, K. Drexler, *Am.j. on addictions* **20**, 485-486 (2011).
28. F. G. Moeller *et al.*, *Am. j.drug and alcohol abuse* **33**, 367-378 (2007).
29. J. Grabowski *et al.*, *J.clin. psychopharmacol.* **15**, 163 (1995).
30. L. P. Cameron *et al.*, *Nature* **589**, 474 (2021).
31. A. G. Nackenoff, A. B. Moussa-Tooks, A. M. McMeekin, J. Veenstra-VanderWeele, R. D. Blakely, *Neuropsychopharmacology* **41**, 1733 (2016).
32. J. Corre *et al.*, *eLife* **7**, e39945. (2018).

ACKNOWLEDGEMENTS

We thank Randy D. Blakely from the Florida Atlantic University Brain Institute for providing SertKI mice. We thank all lab members for suggestions and comments on the experiments and manuscript. We also thank Camilla Bellone, Barry Everitt and Foivos Markopoulos for critical comments on the manuscript.

Funding: This work was supported by the Swiss National Science Foundation and the European Research Council.

Author contributions: Conceptualization: YL, VP, CL; Investigation: YL, LDS, VP; Data analysis: YL, RVZ, JF; Visualization: YL, JF; Reagents: KMN, JXW, FR, YLL, Funding acquisition: CL; Supervision: CL; Writing: YL, VP, CL; Senior authors: YLL, KMN, VP, CL.

Competing interests: Authors declare that they have no competing interests.

Data and materials availability: All data, code, and materials are available on Zenodo at the following address (10.5281/zenodo.5026115).

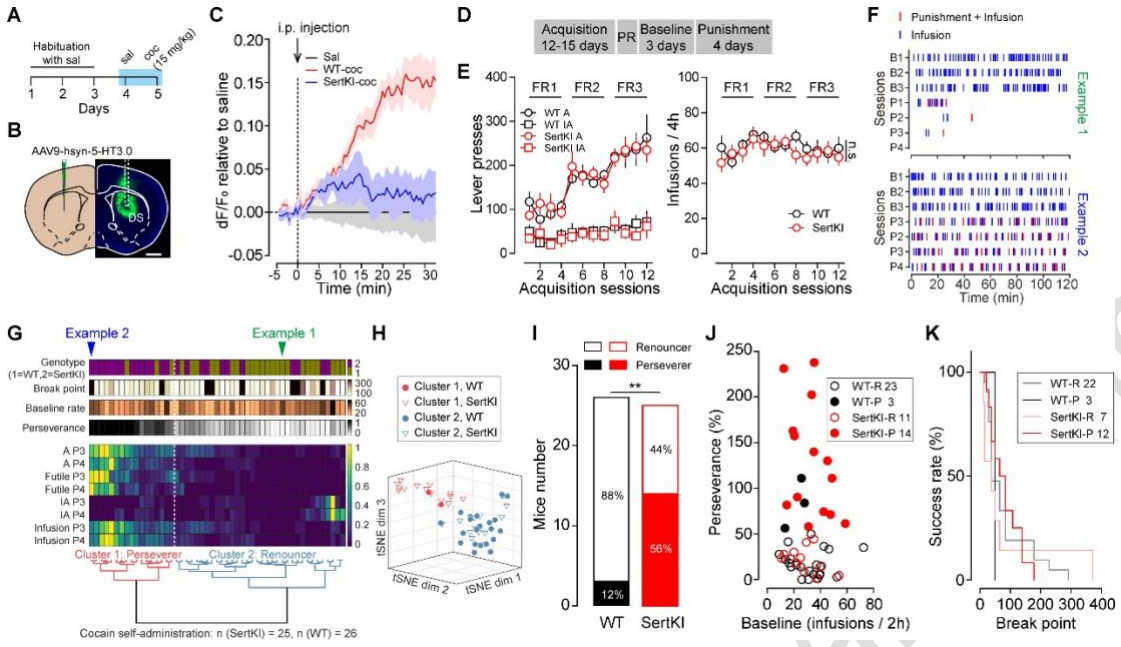

Fig. 1. SertKI animals are more compulsive for cocaine self-administration. (A) Schedule of saline and cocaine injections. **(B)** GRAB 5-HT sensor expression indicated with GFP staining in the DS. Scale bars, 1 mm. **(C)** 5-HT transients in the DS induced by saline / cocaine (15 mg/kg) i.p. injection in WT and SertKI mice (n = 3 mice for WT and SertKI group, data from saline injected WT and SertKI are pooled). **(D)** Timeline of cocaine SA. **(E)** Left, number of active (A) and inactive (IA) lever presses of WT (black) and SertKI (red) animals (n = 26 and 25 for WT and SertKI group) in acquisition sessions. Right, cocaine infusions obtained from WT (black) and SertKI (red) mice in acquisition sessions (two way ANOVA; $F_{1,588}$ = 1.996, P = 0.1583; n = 26 and 25 for WT and SertKI group). **(F)** Raster plots for infusions (blue lines) and punishments (red lines) in baseline and punishment sessions of a renouncer (upper, WT mouse) and a perseverer (lower, SertKI mouse). **(G)** Hierarchical clustering based on tSNE projection of different parameters of punishment sessions 3 and 4 (P3 and P4) of cocaine SA. Blue and green arrow heads indicate examples presented in F. **(H)** tSNE three dimensional representation of clusters of perseverers (cluster 1) and renouncers (cluster 2) in cocaine self- administration. **(I)** Percentage of perseverers and renouncers among WT and SertKI groups (Fisher's exact test; P = 0.001). **(J)** Perseverance rate as a function of baseline rate (Pearson r = -0.08; P = 0.55). **(K)** The success rate of performance as a function of the last progressive ratio value achieved by the mice (logrank test; P = 0.95). Abbreviations, PR, progressive ratio; FR, fixed ratio; A, active lever presses; IA, inactive lever presses; R, renouncer; P, perseverer; sal, saline; coc, cocaine; WT, wildtype; SertKI, SERT Met172 knockin. Data presented as means ± SEM.

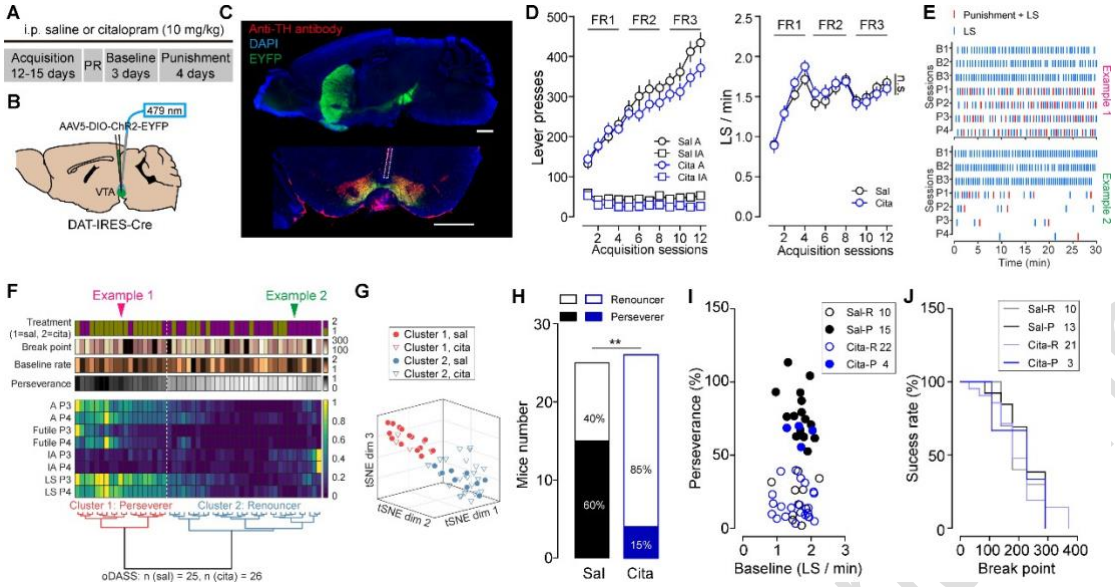

Fig. 2. Citalopram decreases compulsive dopamine self-stimulation. (A) Timeline of oDASS and saline / citalopram treatments. **(B)** Schematic of virus injection sites and optic fiber implantation sites. **(C)** ChR2-EYFP expression in the VTA from a sagittal slice (upper) and a coronal slice co-labeled with TH (lower). Scale bars, 1 mm. **(D)** Left, number of active (A) and inactive (IA) lever presses of saline (black) and citalopram (blue) treated mice (n = 25 and 26 for saline and citalopram group) in acquisition sessions. Right, laser stimulation per minute obtained from saline (black) and citalopram (blue) treated mice in acquisition sessions (two way ANOVA; $F_{1,588} = 0.73$, $P = 0.39$; n = 25 and 26 for saline and citalopram group). **(E)** Raster plots for laser stimulations (blue lines) and punishments (red lines) in baseline and punishment sessions of a perseverer (upper, from saline group) and a renouncer (lower, from citalopram group). **(F)** Hierarchical clustering based on different parameters of punishment sessions 3 and 4 (P3 and P4) of oDASS. Red and green arrow heads indicate examples presented in E. **(G)** tSNE three dimensional representation of clusters of perseverers (cluster 1) and renouncers (cluster 2) in oDASS. **(H)** Percentage of perseverers and renouncers among saline and citalopram treated groups (Fisher's exact test; P = 0.001). **(I)** Perseverance rate as a function of baseline rate (Pearson $r = 0.05$; $P = 0.71$). **(J)** The success rate of performance as a function of the last progressive ratio value achieved by the mice (logrank test; P = 0.95). Abbreviations, LS, laser stimulation; cita, citalopram. Data presented as means ± SEM.

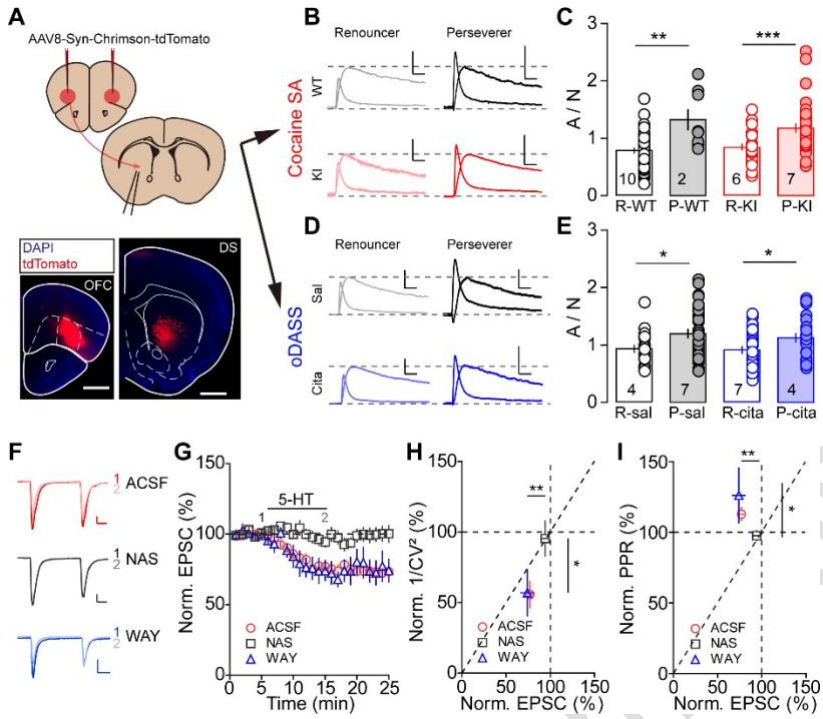

Fig. 3. The OFC-DS pathway is modulated by 5-HT. (A) Upper, Schematic of virus injection and recording sites. Lower, Chrimson-tdTomato expressing cell bodies in the OFC (left) and terminals in the DS (right). Scale bars, 1 mm. **(B)** AMPA and NMDA currents at +40 mV of a renouncer (left) and a perseverer (right) from WT (upper) and SertKI (lower) group after cocaine SA. Scale bars, 200 pA, 15 ms. **(C)** Average A/N of WT and KI renouncers and perseverers after cocaine SA (Mann Whitney test; $U = 74$, $P = 0.003$; $n = 53$ and 8 cells from 10 and 2 mice for renouncer and perseverer in WT group; $U = 252$, $P = 0.0001$; $n = 32$ and 35 cells from 6 and 7 mice for renouncer and perseverer in SertKI group). **(D)** AMPA and NMDA currents at +40 mV of a renouncer (left) and a perseverer (right) from saline (upper) and citalopram (lower) treated group after oDASS. Scale bars, 200 pA, 15 ms. **(E)** Average A/N of saline and citalopram treated renouncers and perseverers after oDASS (two tailed *t* test; $t_{54} = 2.54$, $P = 0.01$; $n = 21$ and 35 cells from 4 and 7 mice for renouncer and perseverer in saline treated group; $t_{55} = 2.38$, $P = 0.02$; $n = 34$ and 23 cells from 7 and 4 mice for renouncer and perseverer in citalopram treated group). **(F)** Traces before and after bath application of 5-HT in the presence of ACSF (red), NAS181 (gray), and WAY100635 (blue). Scale bars, 200 pA, 10 ms. **(G)** Average traces of EPSC before, during and after bath application of 5-HT in the presence of ACSF (red), NAS181 (gray), and WAY100635 (blue) ($n = 13$ and 14 cells from 3 mice for ACSF and NAS181 group, and 7 cells from 4 mice for WAY100635 group). **(H)** Normalized coefficient of variation ($1/CV^2$) versus normalized EPSC (one way ANOVA; $F_{2,31} = 3.682$, $P = 0.0367$ for Norm. $1/CV^2$; $F_{2,31} = 7.948$, $P = 0.0016$ for Norm. EPSC; $n = 13$ and 14 cells from 3 mice for ACSF and NAS181 group, and 7 cells from 4 mice for WAY100636 group). **(I)** Normalized pair pulse ratio (PPR) versus normalized EPSC (Kruskal-Wallis test; $P = 0.041$ for Norm. PPR; $n = 13$ cells from 3 mice for ACSF group, 10 and 6 cells from 2 mice for NAS181 and WAY100636 group). Data presented as means ± SEM.

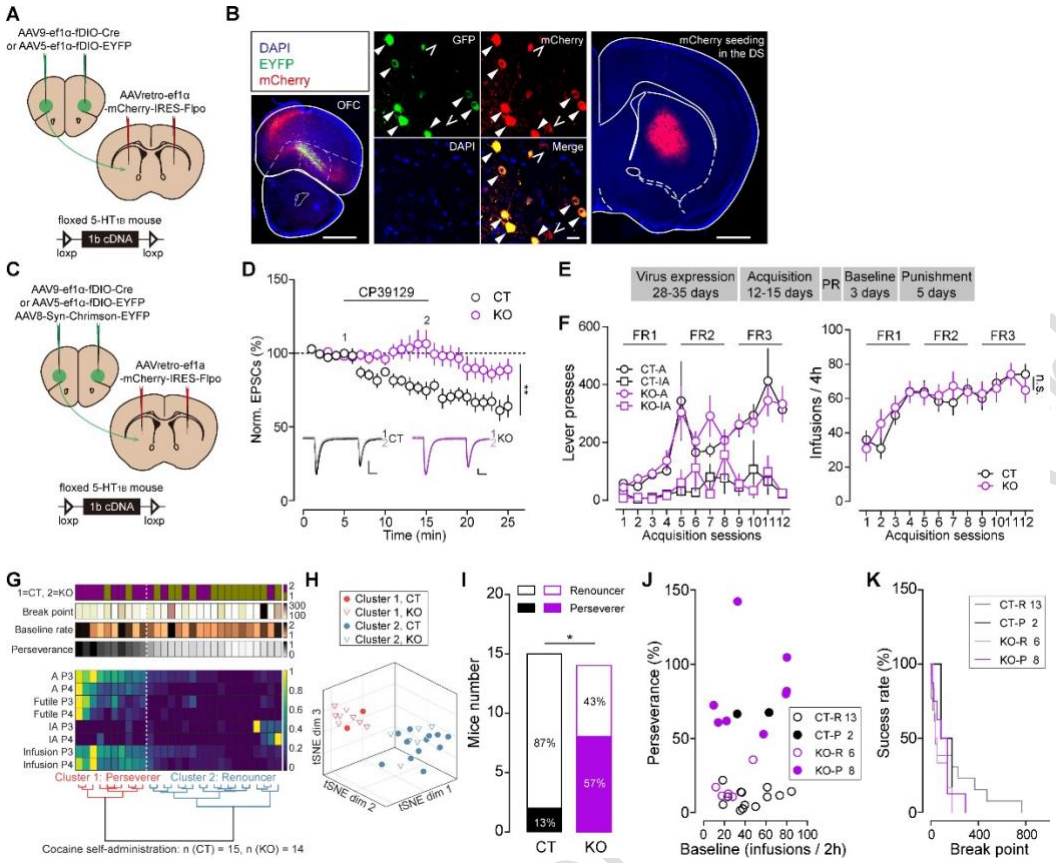

Fig. 4. Knocking out 5-HT$_{1B}$ receptors promotes compulsive cocaine self-administration. (A) Schematic of virus injections for cocaine SA. **(B)** Left and middle, EYFP co-expressing with mCherry in the OFC. Right, mCherry seeding in the DS. Scale bars, 1 mm (left and right), and 20 µm (middle). Arrows indicate DS projectors in the OFC expressing both EYFP and mCherry, open arrows indicate DS projectors expressing mCherry not infected by AAV-fDIO-EYFP. (C) Schematic of virus injections for patch clamp recording. **(D)** Average traces of EPSC before, during and after bath application of 5-HT$_{1B}$ receptor agonist CP39129 in control (CT, black) and pathway specific knockout 5-HT$_{1B}$ receptor (KO, violet) groups (compared Norm. EPSC recorded on last 5 minutes; two tailed *t* test; $t_{25} = 2.86$, $P = 0.008$; $n = 15$ and 12 cells from 3 mice for CT and KO group). Scale bars, 200 pA, 10 ms. **(E)** Timeline of virus injection and cocaine SA experiments. **(F)** Left, number of active (A) and inactive (IA) lever presses of CT (black) and KO (violet) mice in acquisition sessions. Right, cocaine infusions obtained by CT (black) and KO (violet) mice in acquisition sessions (two way ANOVA; $F_{1,324} = 0.198$, $P = 0.66$; $n = 15$ and 14 for CT and KO group). **(G)** Hierarchical clustering based on different parameters of punishment sessions 3 and 4 (P3 and P4) of cocaine SA. **(H)** tSNE three dimensional representation of clusters of perseverers (cluster 1) and renouncers (cluster 2) in cocaine SA. **(I)** Percentage of perseverers and renouncers among CT and KO groups (Fisher's exact test; $P = 0.02$). **(J)** Perseverance rate as a function of baseline rate (Pearson $r = 0.20$; $P = 0.30$). **(K)** The success rate of performance as a function of the last progressive ratio value achieved by the mice (logrank test; $P = 0.84$). Data presented as means ± SEM.

Supplementary Materials for

Synaptic mechanism underlying serotonin modulation of transition to cocaine addiction

Yue Li, Linda D. Simmler, Ruud Van Zessen, Jérôme Flakowski, Jin-Xia Wan, Fei Deng, Yu-Long Li, Katherine M. Nautiyal, Vincent Pascoli, Christian Lüscher*

Correspondence to: christian.luscher@unige.ch

This PDF file includes:

Materials and Methods

Animals

DAT-IRES-Cre (B6.SJL-Slc6a3$^{tm1.1(cre)Bkmn}$/J) mice were used for oDASS experiments. SERT Met172 knockin mice (*10*) on a C57BL/6J background (*31*) from Dr. Randy D. Blakely lab were used for cocaine self-administration experiments. 5-HT$_{1B}$ floxed mice from Dr. Katherine M. Nautiyal lab (*17*) were used for 5-HT$_{1B}$ receptor knock out experiments. D1-tdTomato (B6.Cg-Tg(Drd1a-tdTomato)6Calak/J) and C57BL/6J mice were used for electrophysiology studies. SERT-Cre mice (B6.129(Cg)-Slc6a4$^{tm1(cre)Xz}$/J) were used for optogenetic activation of DR 5-HT neurons. Both male and female mice at the age of 6-20 weeks were used. Mice were food deprived 12 hours before the first session of oDASS and cocaine self-administration. 5-HT$_{1B}$ floxed mice were mildly food restricted (body weight kept above 90% of baseline) during all sessions of cocaine self-administration. In other conditions, food and water were provided ad libitum. Mice were single housed after surgery. All mice were housed at a constant temperature and humidity with a 12-h light/dark cycle. All procedures were approved by the Institutional Animal Care and Use Committee of the University of Geneva and by the animal welfare committee of the Canton of Geneva.

Stereotaxic injections

6-8 weeks old mice were deeply anesthetized using 5% Isoflurane (w/v) and placed in a stereotaxic apparatus (Angle One). Anesthesia was maintained with 2% Isoflurane. Lacryvisc (Alcon, Switzerland) was applied to prevent the eyes from drying. Lidocaine was applied on the surface of the epicranium. An incision was made to expose the bregma and lambda point of the skull. The skull above the target area was thinned with a dental drill and carefully removed. Viruses were injected with glass pipette at a rate of 50 nl/min. The amount of virus per injection site was 350-500 nl. After injection, the pipette was left in the place for 10 min to allow diffusion of the virus. The skin was sutured and disinfected after the injection. 500 µl saline was i.p. injected. Paracetamol (2 mg/ml in the water bottle) was given orally for the next 2-4 days.

To express opsins in the VTA, AAV5-ef1α-DIO-ChR2(H134R)-EYFP (UNC) was injected with the coordinates: anterior-posterior (AP) -3.3; medial–lateral (ML) +0.9 with a 10° angle; dorsal-ventral (DV) -4.3. To express opsins in the OFC, AAV8-hsyn-Chrimson-tdTomato (UNC) was injected bilaterally with the coordinates: AP +2.6, ML ±1.65, DV -2.25. To express GRAB 5-HT sensor in the DS, AAV9-hSyn-5-HT3.0 from Yu-Long Li lab was injected unilaterally with the coordinate: AP +0.8; ML-1.8; DV -3.3. To express opsins in the DRN, AAV8-syn-Flex-Chrimson-tdTomato (UNC) were injected with the coordinate: AP -4.2, ML +0.6 with a 10° angle, DV -3.05. To knock down 5-HT$_{1B}$ receptors in the OFC-DS pathway, retroAAV-ef1α-mCherry-IRES-Flpo (RRID: Addgene_55634) was injected in the DS and AAV9-ef1α-fDIO-Cre (RRID: Addgene_121675) was injected in the OFC.

For oDASS and fiber photometry experiments, optic ferrules were placed 0.2 mm above the virus injection sites in the VTA or DS immediately after virus injection. Two screws and dental cement were was used to secure the implantation.

Catheter implantation

Mice were anesthetized using a mixture of ketamine (80-100 mg/kg) and xylazine (10 mg/kg) by i.p. injection. Lacryvisc (Alcon, Switzerland) was applied to prevent the eyes from drying. The right lateral part of the neck was disinfected and a small incision of about 5 mm was made above the vein. A small incision was made on the upper back between the shoulders, and the surrounding skin subcutaneous fat was detached. The catheter (model MIVSA, CamCaths) was filled with heparin (Heparin Bichsel®) and its tip was brought under the skin from the back to the incised neck area. The neck vein was carefully isolated and regularly rinsed with saline. A small hole was punched on the vein with a needle, and the tip of the catheter was placed into the vein through this hole. The successful placement was checked by withdrawing blood from the vein. The catheter was stabilized with cotton threads and glue. The catheter was put under the skin and all incisions on the neck and back were sutured and disinfected. 500 µl saline was i.p. injected. Paracetamol (2 mg/ml in the water bottle) was given orally for the next 2-4 days. Antibiotics (Amikin, 1 mg/kg) was injected s.c. for five days to prevent potential infections. Mice were single housed after catheter implantation.

Optogenetic dopamine self-stimulation (oDASS)

The mice were subjected to oDASS protocol adapted from previous publication (*6*, *13*) 4 weeks after recovery from the surgery. Operant chambers (ENV307A-CT, Med Associates) situated in sound-attenuating boxes (Med Associates) were used for operant tasks. The apparatus was controlled and data were captured using MED-PC IV software (Med Associates).

Acquisition:

Mice were food deprived 12 h before the first session. After that the mice had food and water access ad libitum. Each session lasted for 1 h, and started with insertion of two levers. Active lever presses induced a train of laser stimulation following a delay of 5 s predicted with 10 s cue light right above the lever. The laser stimulation composed of 30 bursts separated by 250 ms (each burst consisted of 5 laser pulses of 4-ms pulse width at 20 Hz). Inactive lever presses had no result. Each active lever press leading to laser stimulation was followed by a 20 s time out during which laser stimulation was no longer available. Acquisition consisted of 4-6 sessions with FR1, 4 sessions with FR2, and 4 sessions with FR3 (FR*n* means the mice have to press the active lever *n* times to get one laser stimulation).

Progressive ratio:

After the acquisition, the mice underwent one session of progressive ratio to measure the motivation for oDASS. The session lasted for a maximum of 4 h. The breakpoint was considered to be the last reached reinforced schedule after 40 min without receiving any laser stimulation. The reinforced schedules were: 1, 3, 5, 8, 12, 16, 22, 29, 38, 50, 65, 84, 108, 139, 178, 228, 291, 371, 473, 603, 767, 977, 1243 and 1582.

Punishment:

After the progressive ratio, mice were subjected to 3 sessions of baseline and 4-5 sessions of punishment to measure compulsivity. The baseline sessions were the same as acquisition sessions with FR3 except for restricted access for 0.5 h. The punishment sessions were the same as baseline sessions except the mice received a mild foot shock (0.2 mA, 500 ms) every 3 laser stimulations, that was predicted with a house light cue. Perseverance rate was calculated by dividing the average infusions from the last two punishment sessions by the average infusions during baseline.

Cocaine self-administration

The mice underwent catheter implantation 3 weeks after virus injections, and were subjected to cocaine self-administration 1 week after recovery from the surgery.

The apparatus and procedure were similar to oDASS except that active lever presses resulted to an i.v. infusion of 0.5 mg/ml cocaine (provided by the pharmacy of the Geneva University Hospital) dissolved in saline. Each acquisition session lasted for 4 h, and each baseline and punishment session lasted for 2h.

Hot plate test

The hot plate apparatus was heated to 55°C ± 0.2, after which the mice were placed on the surface of the hot plate equipped with a cylindrical animal restrainer at 25 cm height. The hot plate latency was set as the latency to the first jump / hind paw withdrawal / paw tremble. The cut off was set to 30 s to avoid tissue damage. The baseline was tested as the hot plate latency without any treatment. Citalopram (10 mg/kg) or cocaine (15 mg/kg) were i.p. injected immediately after baseline test, and the second test was conducted 30 min after the injections.

Electrophysiology recording ex vivo

To obtain acute brain slices, the mice were anesthetized with 5% isoflurane. The mice were decapitated and the brain was quickly removed and placed in cold oxygenated artificial cerebrospinal fluid (ACSF) containing (in mM): NaCl 119, KCl 2.5, $MgCl_2$ 1.3, $CaCl_2$ 2.5, Na_2HPO_4 1.0, $NaHCO_3$ 26.2 and glucose 11. 220 µm coronal slices containing the DS were prepared with a vibratome (Leica, VT1200). The slices were allowed to recover in 30 °C oxygenated ACSF for 15 min and maintained at room temperature.

For patch clamp recordings, slices were kept at 30 °C in a recording chamber perfused with 2.5 ml/min ACSF. Neurons were visualized with a fluorescent microscope (Olympus BX50WI). Signals were amplified (Multiclamp 700B, Axon Instruments), filtered at 5 kHz and digitized at 20 kHz (National Instruments Board PCI-MIO-16E4, Igor, Wave Metrics). Data were rejected if the access resistance changed more than 20%. EPSCs were evoked with 2 ms orange LED (ThorLabs), and recorded in the presence of PTX (100 µM, Tocris).

AMPA/NMDA (A/N) ratio and rectification index (RI) were recorded with an internal solution containing (in mM): CsCl 130, NaCl 4, creatine phosphate 5, $MgCl_2$ 2, NA_2ATP 2, NA_3GTP 0.6, EGTA 1.1, HEPES 5, QX-314 5, and spermine 0.1. A/N ratio was calculated by dividing AMPA currents isolated with AP5 (50 µM) to NMDA currents obtained by subtracting AMPA component from recordings at +40 mV. RI was calculated as the ratio of the chord conductance calculated at -70 mV divided by chord conductance at +40 mV. Serotonin induced LTD were recorded with an internal solution contained (in mM): potassium gluconate 140, $MgCl_2$ 2, KCl 5, Na_2ATP 4, Na_3GTP 0.3, creatine phosphate 10, HEPES 10 and EGTA 0.2. Strontium mediated qEPSCs were measured by replacing Ca^{2+} with Sr^{2+} in the ACSF. Unitary events were recorded between 10 ms to 100 ms after the light pulse with the internal solution containing (in mM): potassium gluconate 140, $MgCl_2$ 2, KCl 5, Na_2ATP 4, Na_3GTP 0.3, creatine phosphate 10, HEPES 10 and EGTA 0.2. All recordings were conducted with PTX (100 µM, Tocris) in the bath.

Immunostaining

Brains were fixed with 4% paraformaldehyde (PFA) for at least 24 h and sliced with vibratome (Leica, VT1200). 50 µm thick slices were washed with 3 times PBS for 5 min and blocked with 10% bovine serum albumin (BSA) dissolved in 0.5% TritonX-100 for 1 hour at room temperature. Slices were incubated with primary antibodies dissolved in blocking buffer overnight at 4 ℃, followed by 4 times 15 min wash with PBS at room temperature. After that, slices were incubated with fluorescent-conjugated secondary antibodies dissolved in blocking buffer for 2 h at room temperature followed by 4 times 15 min wash with PBS. Last, slices were mounted using mounting medium containing DAPI (Fluoroshiel, Abcam). Primary and secondary antibodies are listed below:
Rabbit anti GFP (1:500, Invitrogen, A11122, RRID: AB_221569); Rabbit anti 5-HT (1:1000, Immunostar, 20080, RRID: AB_572263); Mouse anti TH (1:500, SIGMA, T2928, RRID: AB_477569); Goat anti Rabbit 488 (1:500, Invitrogen, A11008, RRID: AB_143165); Donkey anti Mouse Cy3 (1:500; Jackson, 715-165-150, RRID: AB_2340813).

Fiber photometry

Recordings

Fiber photometry was performed similar to before (*32*). Briefly, 5-HT3.0 sensor was excited using two excitation sources corresponding to 470 nm wavelength (M470F3, Thorlabs) and 405 nm wavelength (M405FP1, Thorlabs) LED light. Both LED lights were sinusoidally modulated at 211 and 531 Hz (470 nm and 405 nm light, respectively) and light was passed through excitation filters (FMC4_AE(405)_E(450-490)_F(500-550)_S) onto an optic fiber patch cable (MFP_400/430/1100–0.48_4 m_FC-ZF2.5, Doric Lenses) that was connected to the chronically implanted fiber (MFC_400/430-0.48_6mm_ZF2.5(G)_FLT, Doric Lenses). Light intensity at the tip of the patch cable was around 0.25 mW. 5-HT3.0 sensor emission light travelled back through the same fibers onto a photo-receiver (Newport 2151, Doric Lenses), after which it was digitized, demodulated and stored using a signal processor (RZ5P, Tucker Davis Technologies). The sample rate was 101.725 Hz, signals were low-pass filtered online at 3 Hz.

For recording DS 5-HT transients elicited by cocaine and citalopram in Fig.1A to C and figS1D, mice were habituated with handling and saline i.p. injection in a circular corridor for three days. On the next days, 5-HT dynamics were recorded 10 min baseline, followed by an i.p. injection of saline or cocaine (15 mg/kg) or citalopram (10 mg/kg), and 40 min recordings afterward.

For recording DS 5-HT transients induced by optogenetic activation of DR 5-HT neurons in figS1A to C, mice were placed in a circular corridor and connected to orange laser (593 nm) as well as the fiber photometry set up. Master-8 was used to control the laser and send markers to the fiber photometry signal processor simultaneously. 5-HT dynamics were recorded before, during, and after the laser stimulation (5-ms pulse width at 20 Hz for 10 s).

Analysis

Fiber photometry signals were analyzed offline in Matlab (Mathworks). To calculate dF/F_0, the signal originating from the 405 nm excitation light was linearly regressed to the signal originating from the 470 nm excitation light. It was then subtracted to create a dF/F_0 using the following formula: (470 nm signal – fitted 405 nm signal)/fitted 405 signal. The average dF/F_0 signal in the baseline periods before experimental intervention was then subtracted to normalize the signal to baseline. Finally, the normalized signal was binned into appropriate time bins in the graphs and analyses.

Clustering analysis

Clustering analysis was performed with Matlab (Mathworks). Prior to the clustering, the variables during the punished sessions (P3 and P4) of each mouse were normalized to the mean signal during the baseline sessions (B1 to B3). The variables used depended on the experiment: cocaine self-administration (active lever presses, futile lever presses, inactive lever presses, infusions) and oDASS (active lever presses, futile lever presses, inactive lever presses, laser stimulations). Futile lever presses reflecting impulsion were defined as the active lever presses during the 20 s time out following the active lever

presses leading to laser stimulations or cocaine infusions. A dimension reduction (Matlab function ‘tsne’ with option algorithm = exact, distance = seuclidean, numDimension = 3) was applied to the variables followed by a hierarchical clustering method (Matlab functions 'pdist', 'linkage' and 'cluster' with a metric = seuclidean and linkage = ward). Since the tsne is a stochastic method, the dimension reduction and clustering were ran 1000 times and the best tree was taken based on the clustering robustness, namely the mean silhouette score was the highest for two clusters (>0.75 over 1, Matlab function ‘silhouette’ for clustering accuracy) and the Cophenetic distance (>0.75 over 1, Matlab function ‘cophenet’ for tree construction accuracy). Finally, other relevant variables were sorted according to the obtained clustering (genotype or treatment, break point, baseline rate and perseverance).

Data analysis

Statistical analyses were performed with GraphPad Prism 6. One-way ANOVA, two-way ANOVA, or two tailed *t* tests were used to analyze data when applicable. Nonparametric test were used if data don’t meet Gaussian distribution. All of the statistical details were presented in the figure legends. Data were presented as means ± standard errors of the means (SEM). Significance was defined as $*P < 0.05$, $**P < 0.01$, and $***P < 0.001$. Sample size were chosen according to previous publications (*6, 13*). Mice were randomly assigned to treatments and conditions. Investigators were blind to genotypes and behavioral outcomes. Electrophysiology data were replicated by 3 investigators in the lab. Behavioral data were replicated at least 3 batches of animal.

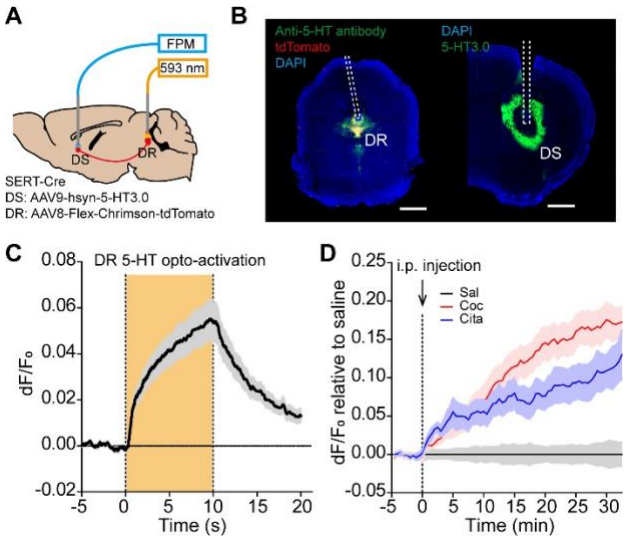

Fig. S1. Validation of GRAB 5-HT sensor. (A) Schematic of virus injection, stimulation, and recording sites. **(B)** Left, Chrimson-tdTomato (red) expression co-labled with 5-HT (green) in the dorsal raphe (DR). Right, GRAB 5-HT sensor expression in the dorsal striatum (DS). Scale bars, 1 mm. **(C)** 5-HT transients recorded in the DS while opto-activating DRN serotonergic neurons (*n* = 3 mice). **(D)** 5-HT transients in the DS induced by saline, cocaine, and citalopram i.p. injection in WT mice (*n* = 6, 6 and 5 mice for saline, cocaine and citalopram group).

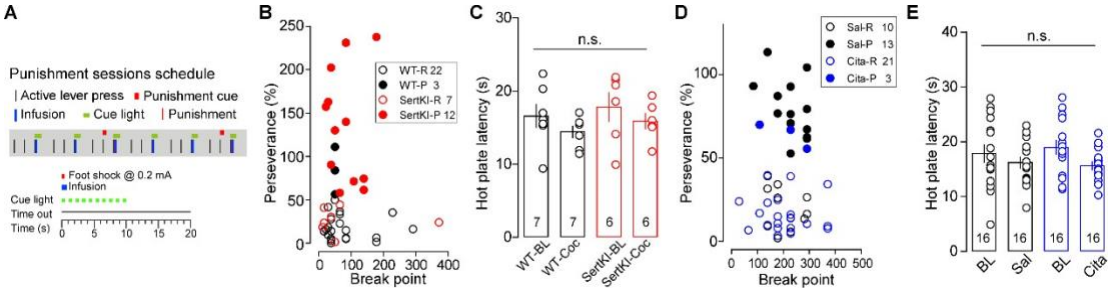

Fig. S2. Lack of correlation between perseverence and breakpoint; no effect on pain perception in cocaine SA and oDASS (A) Schedule of punishment sessions of cocaine self-administration. **(B)** Perseverance rate as a function of break point in cocaine self-administration (Pearson r = -0.01; P = 0.93). (**C)** Hot plate latency of WT and SertKI group before (BL) and after cocaine (15 mg/kg) i.p. injection (one way ANOVA; $F_{3,22}$ = 1.031, P = 0.398; n = 7 and 6 for WT and KI group). **(D)** Perseverance rate as a function of break point in oDASS (Pearson r = 0.02; P = 0.92). **(E)** Hot plate latency before (BL) and after saline or citalopram (10 mg/kg) i.p. injection (Kruskal-Wallis test; P = 0.28; n = 16 for each group).

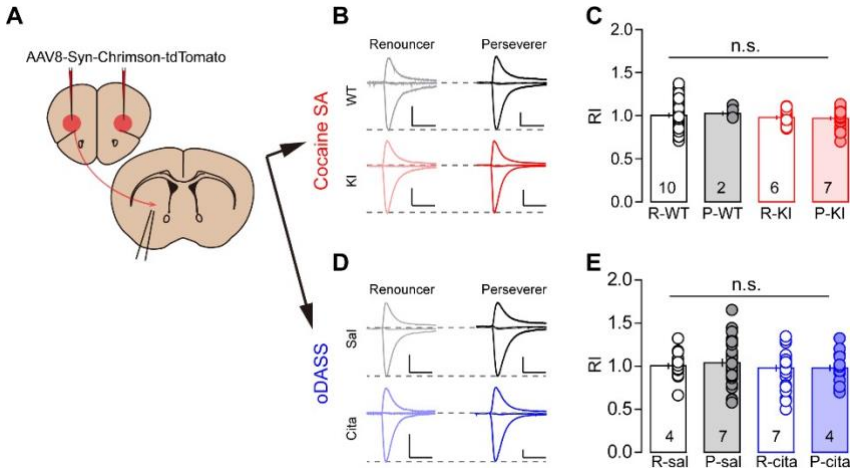

257

258 **Fig. S3. Absence of Rectification of AMPA Epscs in renouncers and perseverers.**
259 **(A)** Schematic of virus injection and recording sites. **(B)** Representative traces of
260 AMPA current holding at -70 mV, 0 mV and +40 mV of a renouncer (left) and a
261 perseverer (right) from WT (upper) and SertKI (lower) treated group of cocaine self-
262 administration. Scale bars, 200 pA, 20 ms. **(C)** Average rectification index (RI) of
263 renouncers and perseverers in cocaine self-administration (WT group: Mann Whitney
264 test; U = 138, P = 0.42; n = 49 and 7 cells from 10 and 2 mice for renouncer and
265 perseverer; SertKI group: two tailed t test; t_{58} = 0.44, P = 0.66; n = 27 and 33 cells from
266 6 and 7 mice for renouncer and perseverer). **(D)** Representative traces of AMPA current
267 holding at -70 mV, 0 mV and +40 mV of a renouncer (left) and a perseverer (right)
268 from saline (upper) and citalopram (lower) treated group of oDASS. Scale bars, 200
269 pA, 20 ms. **(E)** Average RI of renouncers and perseverers in oDASS (saline treated
270 group: Mann Whitney test; U = 320, P = 0.53; n = 21and 34 cells from 4 and 7 mice
271 for renouncer and perseverer; citalopram treated group: two tailed t test; t_{54} = 0.004, P
272 = 0.996; n = 33 and 23 cells from 7 and 4 mice for renouncer and perseverer).
273
274

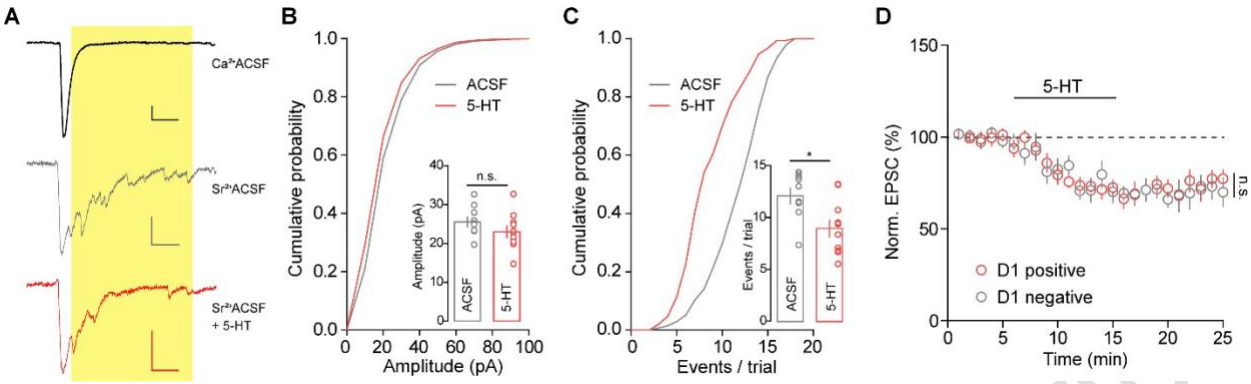

Fig. S4. Modualtion of OFC-DS pathway by 5-HT. (A) Representative traces of evoked EPSC (upper, black) in calcium based ACSF and qEPSC with (middle, gray) and without (lower, red) 5-HT application in strontium based ACSF. Scale bars, 100 pA, 20 ms. **(B)** Cumulative probability of qEPSC amplitude (two tailed *t* test; t_{17} = 1.278, P = 0.218; n = 9 and 10 cells from 3 mice). **(C)** Cumulative probability of qEPSC events/trial (two tailed *t* test; t_{17} = 2.762, P = 0.013; n = 9 and 10 cells from 3 mice). **(D)** Average traces of EPSC before, during and after bath application of 5-HT in D1 positive (red) and negative (gray) cells (compared Norm.EPSC recorded on last 5 minutes; two tailed *t* test; t_{23} = 0.33, P = 0.75; n = 13 and 12 cells from 5 mice for D1 positive and negative groups).

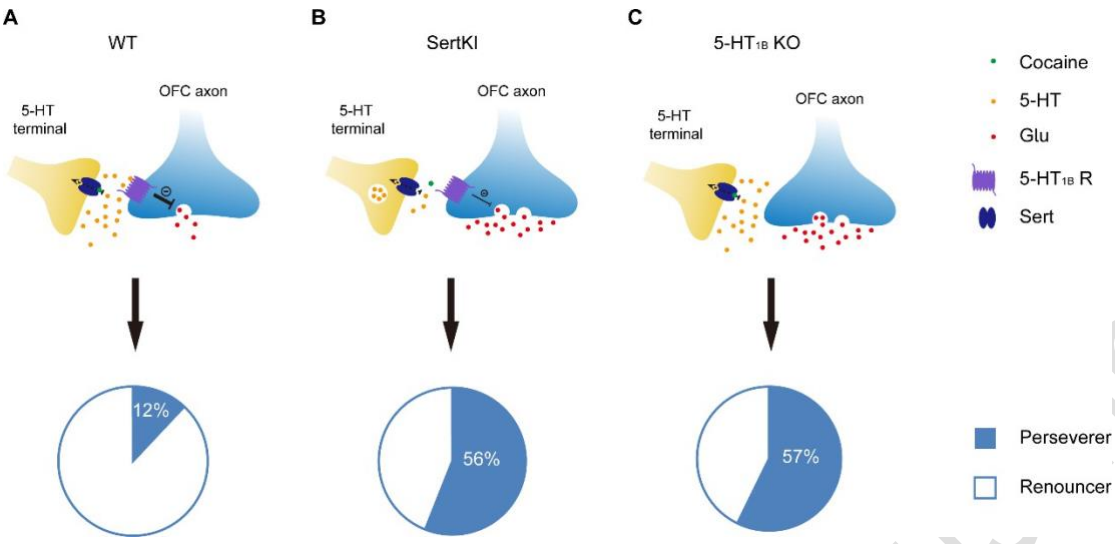

287

288 **Fig. S5. Schematics of working model. (A)** In WT mice, when cocaine binds to 5-HT
289 transporter (SERT), 5-HT reuptake is inhibited and extracellular 5-HT level is elevated.
290 Elevated 5-HT strongly inhibits glutamate release from OFC terminals within the DS
291 through activating presynaptic $G_{i/o}$ coupled 5-HT_{1B} receptors. Weakened OFC-DS
292 synapse results in low fraction of mice to compulsively self-administrate cocaine
293 despite punishment. **(B)** In SertKI mice, in which cocaine cannot bind to SERT, 5-HT
294 level are not elevated by cocaine infusions during cocaine self-administration. The
295 excitatory neural transmission between OFC and DS in SertKI mice is more efficient
296 than in WT mice, leading to higher fraction of perseverers. **(C)** In 5-HT_{1B} KO mice,
297 although cocaine still inhibits 5-HT reuptake and induce elevated extracellular 5-HT
298 level, 5-HT cannot inhibit OFC-DS transmission because of a lack of presynaptic 5-
299 HT_{1B} receptors. The transmission between OFC and DS is strong and promotes
300 transition to compulsive cocaine self-administration.

301

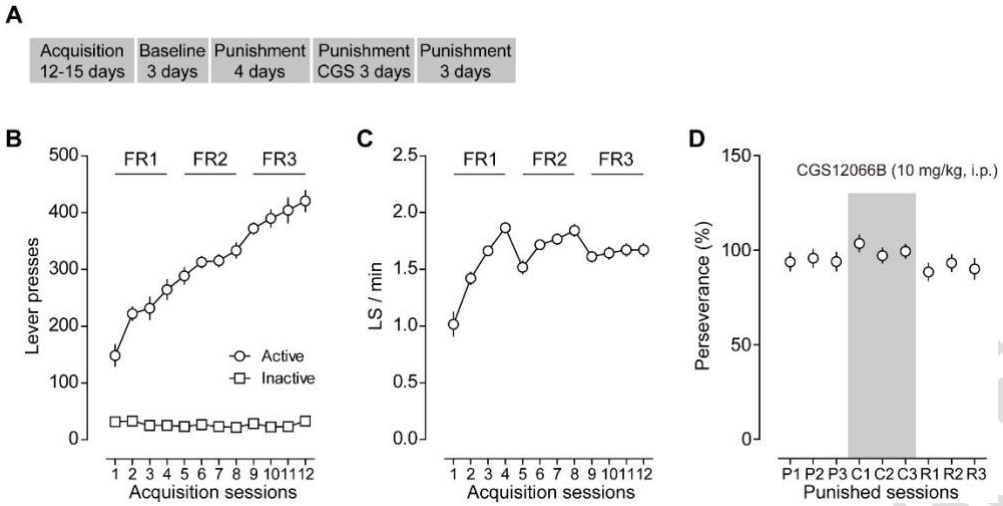

Fig. S6. 5-HT$_{1B}$ agonist treatment in persevering mice after punishment left oDASS unaffected. (A) Time line of oDASS and 5-HT$_{1B}$ agonist (CGS12066B, 10 mg/kg, i.p.) treatment. **(B)** Number of active and inactive lever presses in acquisition sessions of oDASS (n = 15 mice). **(C)** Laser stimulation per minute in acquisition sessions (n = 15 mice). **(D)** Perseverance rate in the last 3 punished sessions (P1-3), punished CGS12066B treatment sessions (C1-3), and additional punished recovery sessions after the treatment (R1-3) (repeated one way ANOVA followed by Dunnett's test; for three consecutive comparisons: q_{14} = 3.04, P = 0.02; q_{14} = 0.89, P = 0.88; q_{14} = 1.66, P = 0.37; and q_{14}= 2.02, P = 0.20; q_{14} = 0.44, P = 0.99; q_{14} = 1.48, P = 0.49 for punished versus punished CGS sessions and punished versus punished recovery sessions, respectively; n = 15 mice).

315 **References**

316

317 31. A. G. Nackenoff, A. B. Moussa-Tooks, A. M. McMeekin, J. Veenstra-
318 VanderWeele, R. D. Blakely, Essential Contributions of Serotonin Transporter
319 Inhibition to the Acute and Chronic Actions of Fluoxetine and Citalopram in
320 the SERT Met172 Mouse. *Neuropsychopharmacology : official publication of*
321 *the American College of Neuropsychopharmacology* **41**, 1733-1741 (2016).
322 32. J. Corre *et al.*, Dopamine neurons projecting to medial shell of the nucleus
323 accumbens drive heroin reinforcement. *eLife* **7**, (2018).

324